



저작자표시-비영리-변경금지 2.0 대한민국

이용자는 아래의 조건을 따르는 경우에 한하여 자유롭게

- 이 저작물을 복제, 배포, 전송, 전시, 공연 및 방송할 수 있습니다.

다음과 같은 조건을 따라야 합니다:



저작자표시. 귀하는 원저작자를 표시하여야 합니다.



비영리. 귀하는 이 저작물을 영리 목적으로 이용할 수 없습니다.



변경금지. 귀하는 이 저작물을 개작, 변형 또는 가공할 수 없습니다.

- 귀하는, 이 저작물의 재이용이나 배포의 경우, 이 저작물에 적용된 이용허락조건을 명확하게 나타내어야 합니다.
- 저작권자로부터 별도의 허가를 받으면 이러한 조건들은 적용되지 않습니다.

저작권법에 따른 이용자의 권리는 위의 내용에 의하여 영향을 받지 않습니다.

이것은 [이용허락규약\(Legal Code\)](#)을 이해하기 쉽게 요약한 것입니다.

[Disclaimer](#)

공학석사학위논문

**전반사 레이저 유도 형광을 이용한
연료 액막 계측에 관한 연구**

**Study on the Measurement of the Liquid Fuel Film
Using Laser Induced Fluorescence
with Total Internal Reflection**

2018 년 2 월

서울대학교 대학원

기계항공공학부

이 재 엽

전반사 레이저 유도 형광을 이용한 연료 액막 계측에 관한 연구

Study on the Measurement of the Liquid Fuel Film
Using Laser Induced Fluorescence
with Total Internal Reflection

지도교수 민 경 덕

이 논문을 공학석사 학위논문으로 제출함

2018 년 2 월

서울대학교 대학원

기계항공공학부

이 재 엽

이재엽의 공학석사 학위논문을 인준함

2018 년 2 월

위 원 장 김 민 수 (인)

부위원장 민 경 덕 (인)

위 원 송 한 호 (인)

Abstract

Study on the Measurement of the Liquid Fuel Film Using Laser Induced Fluorescence with Total Internal Reflection

Jaeyeop Lee

Department of Mechanical and Aerospace Engineering
The Graduate School
Seoul National University

Direct Injection Spark Ignition (DISI) engine has taken advantages of high volume efficiency and high compression ratio caused by the charge-cooling effect. These make it possible to equip a smaller engine into a vehicle while maintaining output. As a result, CO₂ emissions is suppressed because the fuel consumption efficiency is advanced by reducing heat loss and weight reduction. With these advantages, the application of direct injection engines is widely spreading. However, non-evaporated droplets and fuel film create localized stoichiometric rich areas which have an adverse effect on combustion such as incomplete combustion and soot emissions. It is necessary to understand the wall film formation and evaporation processes to reduce piston or cylinder wall wetting.

A quantitative measurement of the formation characteristics of fuel liquid film, which is the cause of particulate matter emission in DISI engines, was conducted by using Laser Induced Fluorescence (LIF) method. Total Internal Reflection (TIR) prevents the laser from absorbing into the airborne droplets above the fuel film by

limiting the laser path. Fuel liquid film was measured irrespective of the injection timing. As a result of this study, it is possible to improve the basic understanding of fuel liquid film formation and a guideline can be provided as a basis for fuel film modeling.

While the experiment based on the preceding TIR study was carried out, It has been found that the laser pulse in the path of TIR passes through the fuel film twice. The fuel film absorbs twice as much energy as expected and emits a strong LIF signal that is twice as intensive. Calibration for the quantification using the thickness gauge was carried out and the fuel film was quantified considering the aforementioned facts.

In this study, the distribution of the thickness, which had not been discussed in the previous study, and thickness of the fuel film including the fuel temperature are investigated using LIF. The empirical results of mass, area and the thickness distribution of the fuel film were analyzed to find the condition that has the most significant amount of effect on the formation of the fuel film.

Injection pressure and split injection do not have a great effect on the fixed system. An elevated changes in the temperature of the fuel seems to have a significant effect on the fuel film formation characteristics. It is discovered that the mass and area are reduced by 40~50%, and a uniform thin film is formed when the temperature of fuel rises 30°C to 90°C .

**Keywords: GDI (Gasoline Direct Injection), LIF (Laser Induced Fluorescence),
Wall film measurement, TIR (Total Internal Reflection),**

Student Number: 2016-20704

Contents

Abstract	i
List of Figures.....	vi
List of Tables.....	ix
Nomenclature	x
Chapter 1. Introduction	11
1.1 Background and Motivation.....	11
1.2 Literature Review and Methodology	15
1.2.1 Wall Film Measurement with RIM.....	15
1.2.2 Wall Film Measurement with LIF.....	17
1.2.3 Other Methodology.....	19
1.3 Objectives.....	21
Chapter 2. Experimental setup.....	22
2.1 Injection System.....	22
2.2 Optical Setup for LIF	24
2.3 New Optical Design for TIR.....	29

Chapter 3. Methodology	30
3.1 Confirmation of Effectiveness of TIR.....	30
3.2 Calibration for Quantitative Measurement.....	32
3.3 Image Processing	42
3.3.1 Wall film detection	42
3.3.2 Quantification.....	43
 Chapter 4. Analysis of Liquid Fuel Films	 46
 Chapter 5. Conclusions	 57
 Bibliography	 59
 국 문 초 록.....	 63

List of Figures

Figure 1. Optical surface phenomena in case of a roughened metal plate without (a) and with (b) liquid covering the surface [3].	15
Figure 2. Principle of Laser Induced Fluorescence (Rincon, 2009)	17
Figure 3. Schematic experimental setup [1].....	19
Figure 4. The mount of injector and heating system.....	23
Figure 5 Transmittance graph of fused quartz ("FUSED QUARTZ AVERAGE TRANSMITTANCE CURVES,").....	26
Figure 6. Schematic diagram of the entire experimental setup for LIF with TIR.....	27
Figure 7. Cross-sectional diagram of the side cut fused silica and a laser beam path	29
Figure 8. (a) Fluorescence of gasoline spray without quartz (b) Fluorescence of gasoline spray under non- TIR condition (c) Fluorescence of gasoline spray under TIR condition	31
Figure 9. Side view of the calibration setup for quantitative measurement	34
Figure 10. An example fitting curve of arbitrary pixel	35
Figure 11. Image of LIF signal with (a) same quartz and (b) 1.1 mm thickness quartz as the upper plate	38

Figure 12. The integrated intensity comparison of central area of LIF images from the setup with TIR and without TIR.	39
Figure 13. Diagram of experimental setup for confirming the calibration method ..	41
Figure 14. Normalized volume of fuel film under ASOI 5, 245, 485 ms.....	41
Figure 15. Process of Image processing of liquid fuel film by LIF	45
Figure 16. Normalized mass of the liquid fuel film at impinging angle 90°	46
Figure 17. Distillation curve of the gasoline supplied in this experiment.....	47
Figure 18. Area of the liquid fuel film at impinging angle 90°	48
Figure 19. LIF images of liquid fuel film under injection pressure 100 bar, impinging angle 90°, single injection, (a) fuel temperature 30°C and (b) fuel temperature 90°C.....	49
Figure 20. Volume fraction of liquid fuel film thickness over 30 microns.....	50
Figure 21. Normalized mass of the liquid fuel film at fuel temperature 90°C	51
Figure 22. Area of the liquid fuel film at fuel temperature 90°C.....	51
Figure 23. Volume fraction of liquid fuel film thickness overall thickness.....	52
Figure 24. Injection conditions and ambient conditions that may affect fuel film formation and the conditions controlled in this study (box frame).....	54
Figure 25. Sample images of liquid fuel film under several injection conditions at 90° impinging angle.....	55

Figure 26. Sample images of liquid fuel film under several injection conditions at
30°C fuel (tip) temperature 56

List of Tables

Table 1 Experimental condition for the measurement of the liquid fuel film.....	23
Table 2 Specification of optical setup	25
Table 3 Experimental conditions	28

Nomenclature

DI	Direct Injection
DISI	Direct Injection Spark Ignition
PFI	Port Fuel Injection
CI	Compression Ignition
PM	Particulate Matter
PN	Particle Number
RDE	Real Driving Emissions
RIM	Refractive Index Matching
LIF	Laser Induced Fluorescence
TIR	Total Internal Reflection
UV	Ultraviolet
ASOI	After start of injection

Chapter 1. Introduction

1.1 Background and Motivation

In a modern Direct Injection Spark Ignition (DISI) engine, injection system is designed to inject some kind of fuel, such as gasoline, ethanol or mixture of them, directly into the combustion chamber. DISI engine has taken advantages of high volume efficiency and high compression ratio and knock suppression due to the charge-cooling effect [1, 2] compared to Port Fuel Injection (PFI) without performance degradation. Combined with turbocharging or supercharging technologies, it enables to apply downsizing design, which is known to have high fuel efficiency and low emission. With these advantages the applications of direct injection engines is widely spreading.

However, if an insufficient time for the spray droplets to evaporate completely is given, non-evaporated droplets will create localized stoichiometric rich areas which have an adverse effect on combustion. In order to make the droplet vaporization easier, the size of them should be smaller. High pressure injection is adopted as a solution [3]. This causes another problem because the high-pressure spray may cause the penetration length of the spray to become longer [4]. Liquid fuel impinges on the piston surface or the cylinder surface, leaving fuel deposit on the surfaces. This is also attributed to an adverse effect on combustion. Drake et al show an endoscopic real image from inside an internal combustion engine with characteristic diffusion flames which are significant sources of soot particles [5].

Particulate Matter (PM) emissions that was not a problem in conventional SI engines becomes subject to regulation by SI engines due to DISI. Of course, the

regulations apply only to engines that employ direct injection rather than conventional fuel injection. Regardless of the combustion cycle, the newly introduced regulations are subject to particulate emission restrictions on engines that adopt the Direct Injection (DI) system for fuel supply. For the DI engine, the Euro 5 emission standard requires PM emissions of less than 0.005 g/km for the SI engine as well as the CI engine, and the Particle Number (PN) emissions limit 6×10^{11} #/km for the Euro 6 emission standard from Sept. 2014. Starting in September 2017, Real Driving Emissions (RDE) will be on the market and vehicle manufacturers will have to comply with the strict exhaust conditions [6]. Recent studies have shown that the emissions from cold start of the RDE cycle account for the majority of total emissions, in the study of Choi et al. about 70% of total emissions [7-9]. This is because the piston wall film, which was found to be the source of the PM in the study of Drake et al. [5], is harder to vaporize under cold start conditions [10].

In order to satisfy the exhaust conditions as described above, it is necessary to understand the wall film formation and evaporation processes to reduce piston or cylinder wall wetting. Many researches on spray and fuel film on the wall have been carried out for that purpose. Several methods have been devised to measure the thickness of fuel film of the order of micron. Refractive Index Matching (RIM) and Laser Induced Fluorescence (LIF) technique are the most commonly used methods for investigate fuel films. RIM measure the thickness of the fuel films by the ratio of the scattered light intensity on the rough surface to the wetted surface. The fuel films on the rough surface makes it flatten. It decreases the light intensity scattered on the surface [11]. This method is limited to wall films thinner than the roughness of the quartz surface of the order of 1~10 μ m. Whereas LIF technique requires a plate with polished surface and it can measure much thicker film than RIM [12].

Cho et al. [13] and Alonso et al. [14] exploited Total Internal Reflection (TIR) on the impinging surface to eliminate the effects of droplets in the air. Using these two methods, many parametric studies have been done, including the influence on film thickness of injector types, fuel types, injection pressure, impinging surface temperature, impinging angle and distance. More recently, Schulz et al. systematically studied the influence of injection pressure, back pressure and back temperature on the fuel film and found that fuel film mass decreased under higher back temperature and lower injection pressure [15-17] .

Quantification in the measurement of liquid fuel film is essential and an additional methodology is required. Measuring the deposition of fuel injected from the inside of the engine on the cylinder or piston head is an experiment with high complexity. It is difficult to observe all the surfaces of the cylinders by using the quartz optical engine, and also to analyze the factors affecting the characteristics of the fuel films requires precise designs for experiments. Although it is challenging to simulate the engine conditions perfectly, it is advantageous for the analysis to measure the entire film through the rig experiment. Experiments designed under specific conditions have the implication that they provide verification data for the simulation. The studies on the injection temperature and strategy of the single hole injector have not been conducted and it is worth trying.

Experiments were designed to introduce LIF because LIF is more suitable than RIM for observing fuel film with various thicknesses. Well-designed LIF studies have been carried out, but interferences caused by airborne droplets have occurred and there has been a limitation to slow down the recording time. In order to investigate the relationship between fuel film and spray and to analyze the formation characteristics, it should be observed from the beginning of the impingement. TIR was applied as a solution. A quartz of a considerably large size is required in order to

secure a window size sufficient to cover the area where the fuel film is formed. The design of the quartz was newly proposed to make it easy to apply TIR. However, TIR had a problem inherent in its design. Two LIF signals are emitted because the laser pulse is reflected from the fuel surface. This issue has not been discussed so far. It is worth discussing methodologically about this. An improved analysis method for the thickness distribution as well as an analysis of the total deposit mass needs to be devised.

1.2 Literature Review and Methodology

1.2.1 Wall Film Measurement with RIM

Refractive Index Matching (RIM) is one of the thickness measurement methods developed by Drake et al. [18, 19]. The principle of RIM is on the physical basis of light scattering. In the method using light scattering, a light source, a surface to which a film is adhered, and a camera are required. The thickness of liquid film is derived from the change of image intensity of light scattered on the rough surface. The basic mechanism of RIM is shown as figure 1. The irradiated light is scattered on a uniformly roughened surface and some part of the light is directed to the detector. When the rough surface is covered by the accumulated liquid, the light is not scattered in the area but is reflected as it is. The amount of scattered light decreases, and the brightness recognized by the detector decreases. That is, as the fuel is thickly covered, the amount of light sensed decreases. The detector usually means a camera.

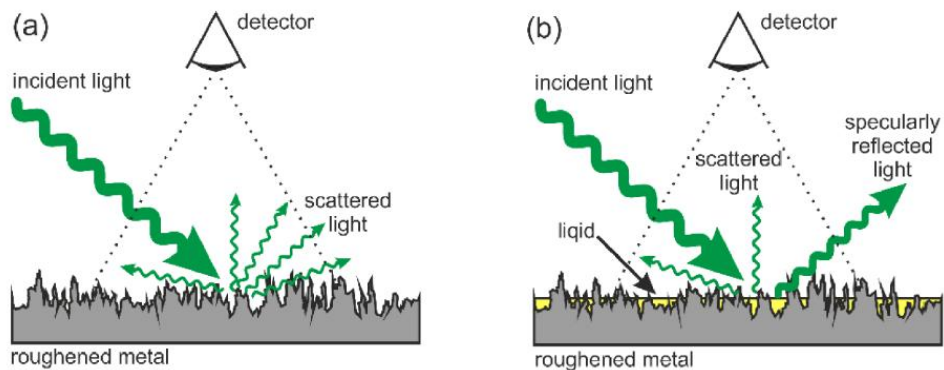


Figure 1. Optical surface phenomena in case of a roughened metal plate without (a) and with (b) liquid covering the surface [3].

In the case of an opaque material surface, the detector and the light source are in the same area based on the surface. For a transparent surface, place the light source on the opposite side of the detector. Even if light is projected in the opposite direction, the result of measuring the quantity of accumulated liquid is on the same trendy [18].

Due to the principle nature of RIM, it is advantageous to apply to low viscosity liquids. Also, there is no influence by kind of liquid. Therefore, it is suitable for measuring the fuel film. Drake et al., Yang et al. and Henkel et al. have also proposed rational and successful calibration methods. [5, 18, 20] However, there is a fatal problem: the greater the thickness of the liquid film than the surface roughness, the exponential decline in accuracy. Their calibration methods were correct, but given the fact that the amount of fuel injected at once is tens of microliters, the values of volume they applied were too small. It is the proof that the correlation in the thick thickness falls. In addition, since it is partially saturated, it is difficult to obtain information on the thickness distribution of the film. The range of allowable volumes is so narrow that it is generally problematic to apply. RIM is a limited method for determining the amount and distribution of fuel films under various conditions.

1.2.2 Wall Film Measurement with LIF

Laser Induced fluorescence is also one of the typical methods of measuring fuel films like RIM. LIF refers to a fluorescent signal emitted by a molecule excited by a laser light source. An explanation of the principle is briefly shown in figure 2. When the ground state molecule absorbs light, it instantaneously becomes S_2 state, which is a high energy level for a very short time. The molecule immediately changes to the lower energy level S_1 state. In this process, physical processes such as radiative processes, non-radiative processes, and collisional quenching occur and energy is lost. The molecule immediately goes down through the S_1 state to the lowest energy state, S_0 (ground state). In this process, radiative emission occurs, that is, a photon is emitted. This radiative emission is observed as fluorescence [21].

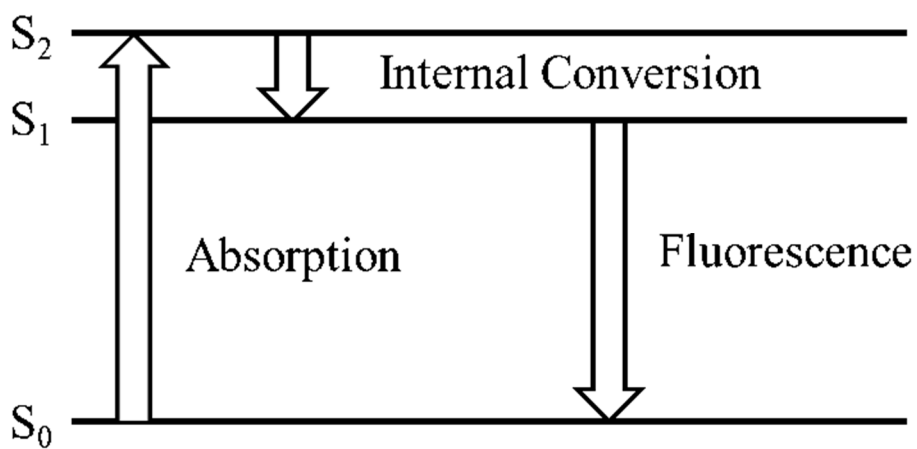


Figure 2. Principle of Laser Induced Fluorescence [22]

In general, wavelength of fluorescence signal of organic molecules is shifted to longer than the wavelength absorbed, called as 'Stokes shifted' [22]. Each material

has a specific wavelength that causes this phenomenon and the light source must match the wavelength to induce sufficient fluorescence to be detected. LIF refers to a laser using a light source.

Most of the LIF studies use substances with good fluorescence as tracers. Typical examples are toluene, acetone, and 3-pentanone. Only components with properties similar to fuel properties remain as suitable tracers. It is almost impossible to find a tracer that perfectly matches fuel and properties. However, the fraction of tracer in fuel mixture is not so high, so it is not a fatal problem. It can also be influenced by temperature and pressure [23, 24]. The injector condition or the environment in which the fuel is injected does not deviate enough to change the tracer's properties. It would not be suitable for use in an engine, but it is not a critical problem in an experimental setup that can control boundary conditions. Also, only the film can be detected by the LIF method coupled with the TIR.

1.2.3 Other Methodology

Recently, a new method has been proposed which uses an infrared camera. A high-resistance metal plate replacing the piston face is heated by current, which is captured by an infrared camera from below. The metal plate is coated with a thin layer of graphite to increase the emissivity. A schematic diagram to help you understand this is shown in figure 3 [25, 26].

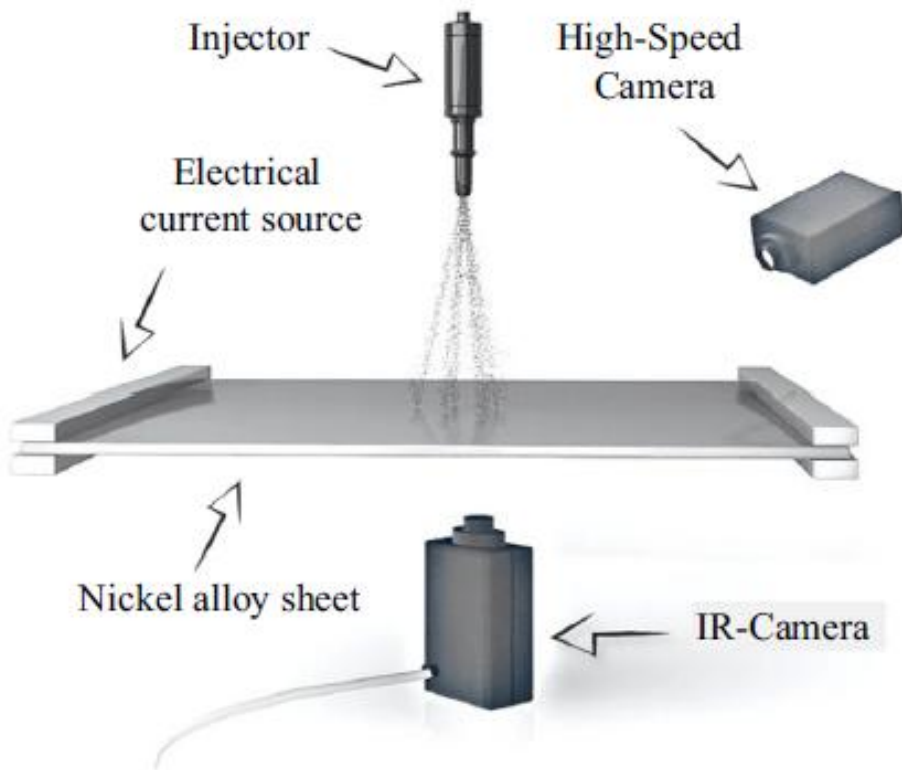


Figure 3. Schematic experimental setup [1]

When impinging on the surface of the fuel heated sheet, the latent heat of the fuel cools the heated sheet. The cooled sheet is taken by the IR camera and the heat flux is calculated by the temperature change over time. From the first law of thermodynamics, the total mass of fuel deposited with the calculated heat flux and time, temperature change, and phase change enthalpy is obtained [25, 27].

This method can be applied irrespective of the kind of fuel if the heat of vaporization of the fuel and specific heat can be obtained. However, high-temperature impact surfaces are known to have a profound effect on spray-wall interaction. Particularly, in the case of gasoline or diesel mixed with a large variety of components, the influence by the surface temperature is greater [28].

1.3 Objectives

The Objectives of this study is to develop a laser fluorescence induction method for quantitatively measuring the fuel film produced by the wall collision of the spray and to provide data for improving the modeling accuracy. In order to achieve these goals, the specific objectives of this study are as follows.

The key objectives of this study can be summarized as follows:

1. Development of a method to observe the liquid fuel film with a non-destructive measurement using Laser Induced Fluorescence (LIF)
2. Development of a method to observe the liquid fuel film formation from the beginning of the collision by coupling Total Internal Reflection (TIR) with Laser Induced Fluorescence (LIF).
3. Design of the rig test setup to mimic the real engine like conditions
4. Analysis of the effect of injection conditions, such as injection pressure, injector tip temperature, split injection and impinging angle, on the formation of liquid fuel films.

Chapter 2. Experimental setup

2.1 Injection System

The gasoline fuel is pressurized by the Haskel pump and injected by the Continental injector. Only one of the 6 holes of the 6-hole injector was preserved, and the others were sealed by laser welding. The injection pressure was set at 100 and 150 bar to account for the influence of the injection pressure in the actual engine. The injection duration was adjusted so that 8.5 mg of the same mass of fuel was injected at each pressure. Injection pressure of 100 and 150 bar, respectively, the injection period of 2.5 ms and 2.07 ms were applied.

A schematic diagram of the injection system is shown in figure 4. The conditions of the system are specified in Table 1. The injector was fixed on the aluminum module with the bar type heaters and placed on the collision wall fused silica. The surface temperature of the fused silica, the tip of the injector, and the injector mounted module were set to K type thermocouples to measure and control the temperature. To avoid unnecessary LIF signal interference, all of the underside of the module was treated with black to reduce reflections. In addition, all surfaces that could cause reflection were covered with black. Experimental results show that the reflection of these surroundings is a major cause of ICCD image noise. Previous studies have also noted that this possibility should be acknowledged and cautioned and beam dumps were installed.

Table 1 Experimental condition for the measurement of the liquid fuel film

Parameter	Condition
Hole type	Single hole (6 holes origin, 5 holes sealed)
Fuel type	Gasoline
Injection mass	8.5 mg
Injection pressure	100 bar, 150 bar
Injection duration	2.5 ms (100 bar), 2.07 ms (150 bar)
Injector tip temperature	30 °C, 90 °C
Tilting angle	45°, 90°
Ambient pressure	1 bar
Ambient temperature	21 °C

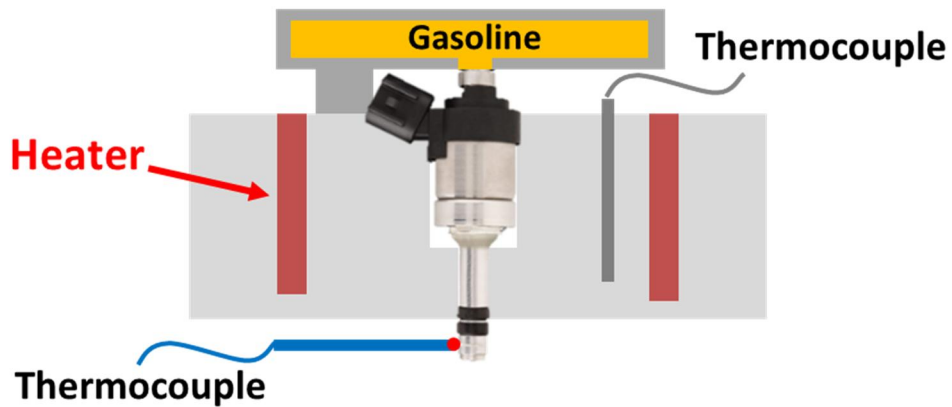


Figure 4. The mount of injector and heating system

2.2 Optical Setup for LIF

Figure 6 shows the entire setup for fuel film LIF experiment. The LIF signal was detected by a high-speed ICCD camera (FASTCAM ultima APX) which has 1,024 gray levels with a resolution of $1,024 \times 1,024$ pixels. By combining the ICCD camera with the Nikon 28-105mm f/3.5-4.5 AF-D NIKKOR lens, a high spatial resolution of $111 \mu\text{m}/\text{pixel}$ was realized. Additionally, a 400 nm long pass filter and a 500 nm short pass filter were mounted to exclude the scattering signal noise generated due to the 2nd harmonic at 532 nm mixed with the 3rd harmonic at 355 nm.

Continuum PL8000 Nd: YAG laser was installed to generate the third harmonic at 355 nm for excitation of gasoline. In this experiment 355 nm laser which had a power of 72 mJ/pulse with a frequency of 10Hz and a pulse duration of 5 to 7 ns was enough to receive the LIF signal of liquid fuel film. From the suggestion of Schulz et al., too much intensity of laser generates a laser-induced plasma causing bubble formation and unwanted modification of emissions. The unintended formation of bubbles brings problems of causing reflection and influencing the film behavior. Homogeneous laser profile and proper intensity of laser intensity should be provided for measuring the fuel film. By setting the laser power to 60 mJ/pulse and adjusting the beam profile, the maximum fluorescence signal could be achieved [17], the laser power used in this experiment is proper to generate LIF signal of liquid fuel film.

The transmittance curve of quartz medium according to the frequency is shown in figure 5. The transmittance curve was the data posted in “Technical Glass Product”. Fused silica is the most profitable material for gasoline LIF because it has a quite high transparency at 355 nm wavelength of light as well as in visible light wavelength range.

The emitted 355 nm laser pulse is reflected by the laser line mirror, passed through the slit, and then expanded by the concave lens. The expanded laser pulse is reflected by the UV mirror at 15 degrees to the horizon and becomes 30 degrees to the ground. The tilted laser pulse is incident on the side of fused silica, which is the wall where the fuel spray collides, and is transmitted to the top surface. It causes total internal reflection at the top of the fused silica and exits through the other side.

When the fuel liquid film formed on the upper surface emits the LIF signal by the laser pulse, it is delivered to the ICCD camera through a 45 degree tilted UV mirror placed underneath the fused silica.

Table 2 Specification of optical setup

Parameter	Specification
Light source	Nd:YAG laser (PL8000)
Wavelength	355 nm
Power variation	4-10%
Imager	1,024 grayscale ICCD
Image processor	FASTCAM ultima APX
Resolution	111 μ m/pixel
Pulse generator	DG535

(Includes Surface Reflection Losses — Samples Tested 10mm Thick)
(Tubing 1mm Thick)

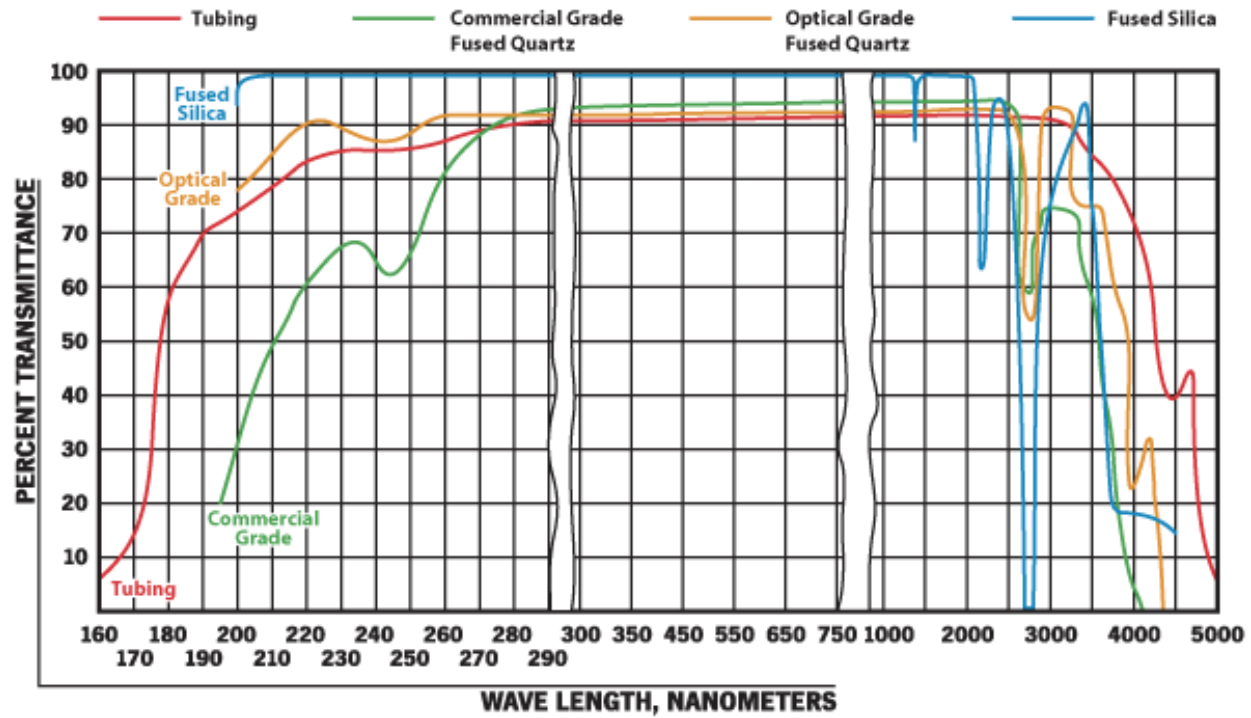


Figure 5 Transmittance graph of fused quartz [29]

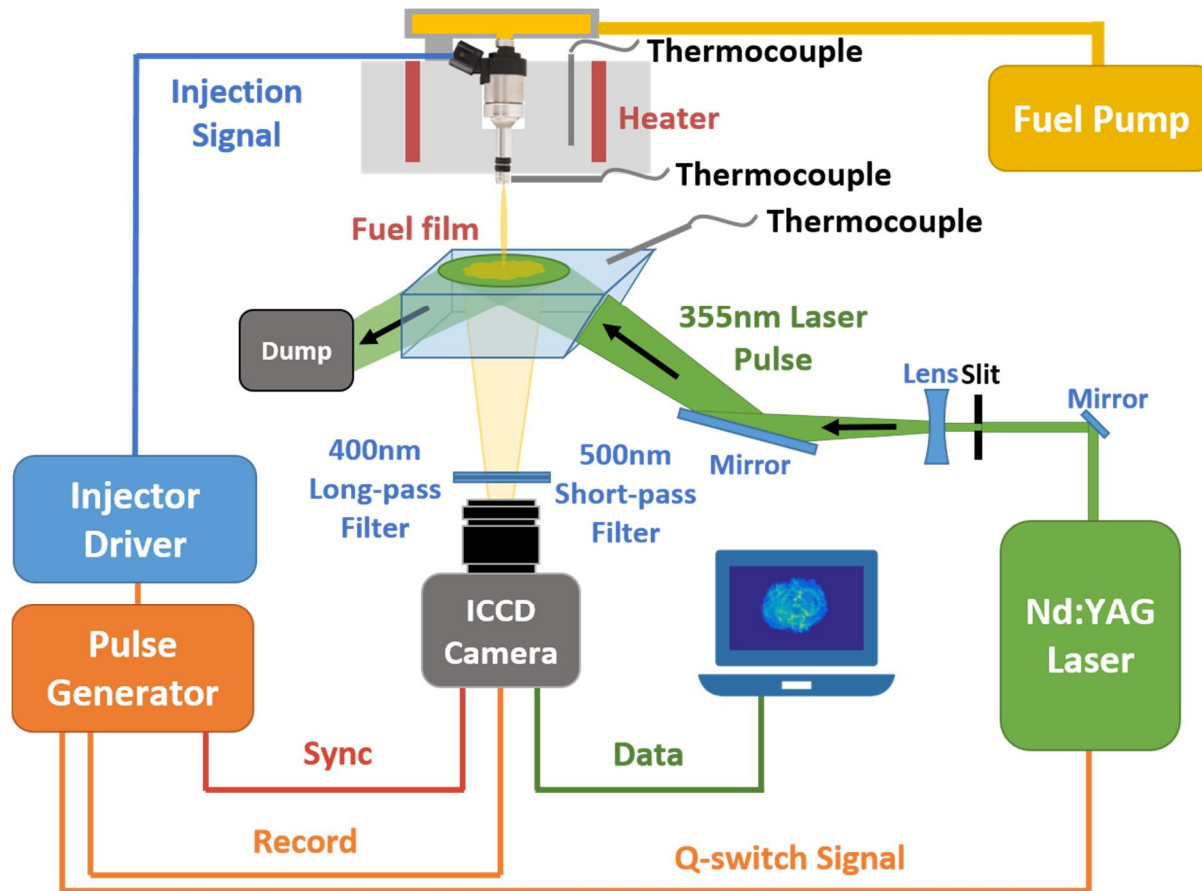


Figure 6. Schematic diagram of the entire experimental setup for LIF with TIR

Table 3 Experimental conditions

Parameter	Conditions
Frame rate	125 fps
Gate	40 μ s
Resolution	256 \times 512 pixels
Laser pulse energy	70mJ
Injection mass	8.5 mg
Injection pressure	100 bar, 150 bar
Injection duration	2.5 ms, 2.07ms
Injector tip temperature	30°C, 90°C
Impinging angle	45°, 90°
Injection strategy	Single : 2.5 ms (100 bar), 2.07 ms (150 bar) Triple : 0.615 – 0.5(dwelling) – 0.473 – 0.5(dwelling) – 0.473 ms (100bar) 0.5 – 0.5 – 0.41 – 0.5 – 0.41 ms (150 bar)
Ambient temperature	21~23°C
Ambient pressure	1 bar
Distance tip to surface	50mm (injection direction)

2.3 New Optical Design for TIR

A new design of impinging plate was devised in this paper. A fused silica of which side was cut by 60 degrees was used as the impinging plate. Previous researchers who applied total internal reflection to the LIF used a quartz plate with a rectangular parallelepiped structure. It does not make any problems to the experiment results, but it costs more because it requires more optical devices. According to the calculation, in order to irradiate a laser beam over a large area of top surface, the thickness of the plate must be very thick as much as the width of plate or some beam shaping cylinder lens must be provided. The more optics require the more accurate arrangement. The new design of fused silica plate of which side was cut by an angle of 30 degrees to make the angle of incidence easier to enter at 60 degrees on the top surface reduced the cost. The comparison of a normal rectangular plate and the side.

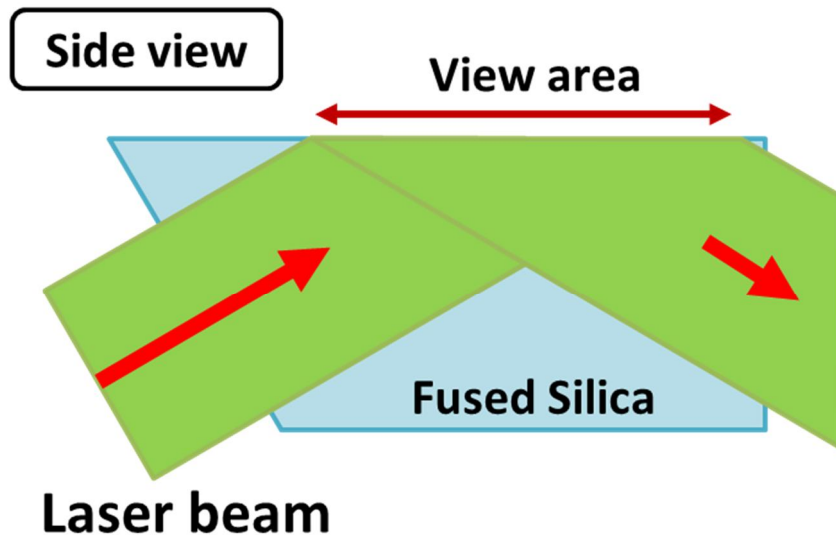


Figure 7. Cross-sectional diagram of the side cut fused silica with a laser beam path

Chapter 3. Methodology

3.1 Confirmation of Effectiveness of TIR

In order to overcome the limitations of the experimental setup of LIF, Kull et al. designed the LIF experiment using total internal reflection in 1997 and successfully filmed the wall film [30]. Using this technique, Cho et al. also made an achievement of measuring liquid fuel film in a visualized engine equipped with a quartz liner [13]. Alonso introduced a total internal reflection into the rig test to capture the fuel injected into the quartz block rather than the visualized engine [14]. However, there has been no evidence to show that air-borne droplets are not actually taken when total internal reflection is introduced. Quantitative comparison of the total reflection effect is very difficult because the density of the laser differs at the incidence angle at which the laser total internal reflection occurs and at the incidence angle which is not. In this study, we tried to compare the spray intensity of the spray under TIR condition and non - TIR condition.

A LIF signal is emitted from the fuel spray at an angle of incidence below the critical angle which is the boundary value of total internal reflection. However, no LIF signal is detected at an angle of incidence over the critical angle. If spray images are taken under the adjusted conditions, the LIF signal is emitted, which means that total internal reflection has not occurred. By comparing the spray images at two laser incident angles, we can confirm that the TIR really has the effect of excluding air born droplets from the LIF. Figure 8 shows the spray images taken based on these assumptions. The effect of TIR was demonstrated in the experimental environment. The spray of the non-total internal reflection condition taken at $f/8$ reliably emitted the LIF signal. Fluorescence was observed irrespective

of After Start of Injection (ASOI). As ASOI was increased, the droplet decreased due to vaporization and the signal was weakened. Figure 8 is an image of a spray taken under TIR conditions. In the early ASOI, the fluorescence of the spray appears a little, but the LIF signal sharply decreases as the ASOI increases. It should be noted that this image is the result of $f/5.6$, so the difference between the two is actually greater. According to the definition of f number, the quantity of light reaching to the camera sensor is doubled from $f/5.6$ to $f/8$. Considering this, the effect of TIR was clear. However, the fluorescence of air born droplets could not be blocked at certain times. Although the error can be reduced compared with the existing experimental method, the problem of overestimation of the fuel membrane cannot be completely solved. This is probably because the surface of the fuel film formed an uneven surface which does not cause total internal reflection due to a large number of droplets.

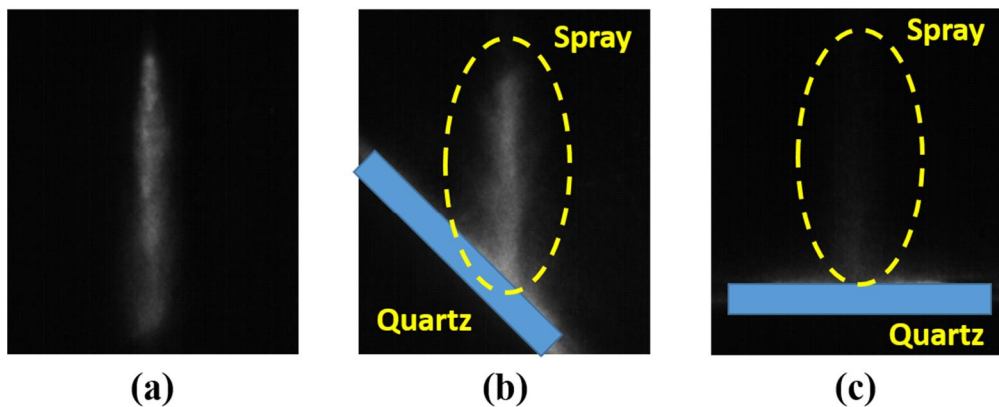


Figure 8. (a) Fluorescence of gasoline spray without quartz (b) Fluorescence of gasoline spray under non- TIR condition (c) Fluorescence of gasoline spray under TIR condition

3.2 Calibration for Quantitative Measurement

The laser-induced fluorescence method used to observe the fuel film utilizes the energy of the irradiated laser absorbed by the atom or molecule and emits the energy again in the form of light.

For the LIF technique, a fluorescent dye or tracer is added to the fuel and the film is illuminated with a known light intensity. However, it is not necessary to add a kind of dye for gasoline because the components that can already act as dyes constitute gasoline.

Fluorescent tracers adjusted to a certain concentration C with a quantum yield Φ and a molar absorption coefficient ε is excited with a defined radiation I_0 . The film thickness is found by measuring the fluorescence intensity I_f . Using the Beer–Lambert law, the film thickness h can be calculated as:

$$I_f = I_0 \Phi (1 - 10^{-\varepsilon Ch}) \quad (3.4.1)$$

Where, I_f : fluorescence intensity
 I_0 : initial laser power
 Φ : quantum yield
 ε : molar absorption coefficient
 C : concentration
 h : film thickness

A closer look at the quantum yield and the absorption coefficient reveals that these can be functions of temperature, pressure and wavelength. In the case of

liquid sample, the effects of temperature and pressure are negligible [12]. It is reasonable to consider that certain concentration C is constant because gasoline is a homogeneous mixture. However, after a long period of time, the components might be separated by gravity, so that the gasoline was sufficiently shaken before the all experiments. The order of film thickness h is $1\sim 10\mu\text{m}$, 10^{-5}mm . The index of 10 of (3.4.1) is very close to zero. Equation (3.4.1) converges to Equation (3.4.2).

$$I_f = I_0 \Phi \epsilon C h \quad (3.4.2)$$

$$I_f / I_0 = \Phi \epsilon C h \quad (3.4.3)$$

$$h = I_f / I_0 \Phi \epsilon C \quad (3.4.4)$$

In equation (3.4.3), all variables except the right h are constants. Finally, the thickness of the fuel film is proportional to the ratio of the intensity of the LIF signal and irradiated laser intensity. If the thickness of fuel film is measured for a fixed induced laser intensity I_0 , the thickness of fuel films can be estimated for a specific brightness by reversing it. Calibration results confirmed the linear relationship between LIF signal and thickness at thin film thicknesses shown as in figure 9. Two gap gauge was placed between the two glasses and gasoline was inserted to make a certain thickness. The gap gauge thickness was gradually increased, and the formed fuel film was irradiated with a laser. The intensity of the single pixel was averaged from 20 cycles to represent the intensity counts corresponding to the generated film thickness.

The calibration curve is presented in figure 10. As a result, it was confirmed that the LIF brightness and thickness showed linearity with R squared value about

0.99. These results are collectively shown for all the pixels in the image. the brightness of each pixel can be reduced to thickness.

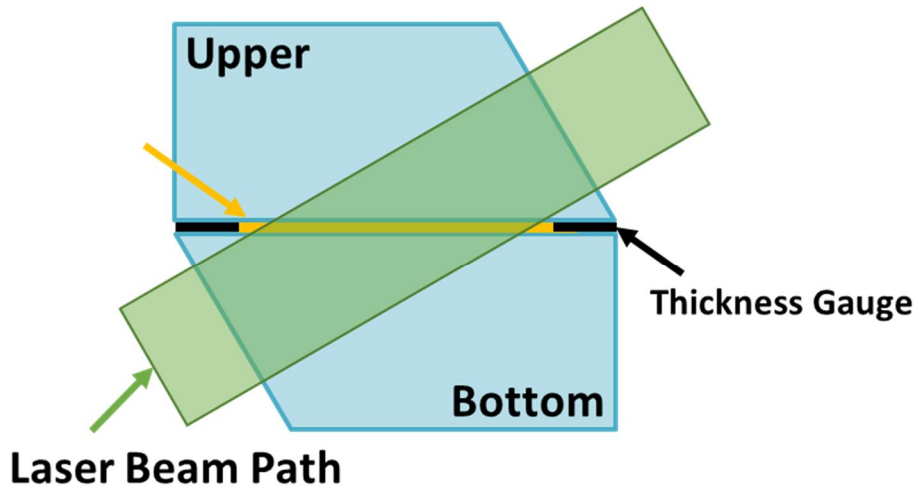


Figure 9. Side view of the calibration setup for the quantitative measurement

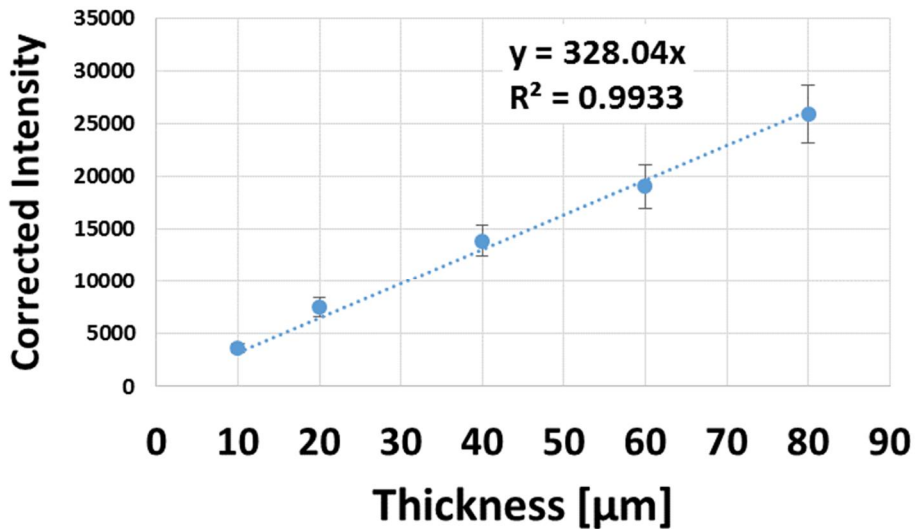


Figure 10. An example fitting curve of arbitrary pixel

In the course of this research, problems were newly found in quantification using TIR. The problem inevitably arises from the principle of TIR. It was not considered in studies using existing TIR.

In the setup to induce TIR, the laser pulse passes through the quartz and reaches the top of the quartz. When there is no fuel, the laser is totally reflected from the upper surface of the quartz and exits to the opposite side. In the case of that the fuel is on the top surface, it is very similar to the refractive index of quartz, so only a little portion of laser pulse is reflected and most of the fuel is transmitted to the fuel on the top surface. Let the LIF signal generated by the fuel absorb the laser as the primary LIF signal. The laser pulse that excited the fuel reaches the top of the fuel film. Due to the difference in refractive index between the fuel and the air, the laser pulse does not advance into the air and the total reflection occurs on the upper surface of the fuel film. The laser pulse thus totally passes through the

fuel film again and enters and exits through the quartz. At this time, the LIF signal is again emitted from the fuel film. Let this signal be a secondary LIF signal.

In this process, the laser has to pass the fuel film twice. In other words, primary and secondary signals inevitably occur. In other studies that do not use TIR, the LIF signal occurs only once because the laser passes through the fuel membrane only once. However, when TIR is applied, the laser fluoresces the fuel again at a shifted position proportional to the cosine of the incident angle and the thickness of the fuel film. Therefore, it is reasonable to assume that the image of the fuel film on which TIR occurs is the summed brightness of both the primary LIF signal and the secondary LIF signal generated by the laser.

Since the thickness of the fuel film is an order of tens of microns, the distance between the primary and secondary LIF signals is approximately 100-150 microns. The difference in the image is at most one pixel which is negligible in this experiment. For each pixel, the value of the secondary LIF values 1 of its own or neighboring pixel is added together. Failure to account for this results in an error measuring over the actual thickness of the fuel film. Alonso's findings indicate that 80 to 90 % of the injection was adhered from fuel injected into the wall at an angle of 45° [22]. The results of this study show that the volume and mass of fuel film formed when the spray impinged at 90 degrees from an angle of 45 degrees or more than 30 %. If he had injected the fuel perpendicular to the impacting surface, he would have faced an inconsistent situation, with a greater amount of adhesion than the quantity injected. This problem does not occur if the laser is totally internally reflected at the top of the fuel film even during the calibration process. A new method is needed to produce a fuel film of uniform thickness without an element covering the fuel film. In all papers using LIF, the conventional method was used. These difficulties prevented us from solving the problems directly.

To solve this problem, several experiments were conducted to verify the hypothesis that the brightness of the entire film should be reduced by a certain factor.

1. It is necessary to confirm whether the brightness of the fuel film is really overestimated by TIR.
2. A certain amount of fuel precisely metered with a micro-syringe was applied to the upper surface of the quartz, and then the theory was applied to examine how much the amount of fuel was equal to the actual fuel amount.
3. It was checked whether the agreement was within a reasonable range.

For the first experiment, the case where only the primary LIF signal is generated should be compared with the case where the secondary LIF signal occurs due to TIR. The setup for calibration was the condition under which only the primary LIF signal was generated. In order to generate the secondary LIF signal, the upper quartz was replaced with a thinner one, so that the laser pulse, which caused the total internal reflection, once again excited the fuel.

TIR was induced to occur as close as possible to the top surface of the fuel film. If the top plate quartz covering the fuel film is very thick, the shifting between the primary LIF signal and the secondary LIF signal becomes large, resulting in overlapping shapes. As thin as possible, the top plate can reduce laser shifting and maximize the overlap effect of the primary LIF signal and the secondary LIF signal. Figure 11 shows an image (a) in which only the primary LIF signal is generated and an image (b) in which the secondary LIF signal is superimposed.

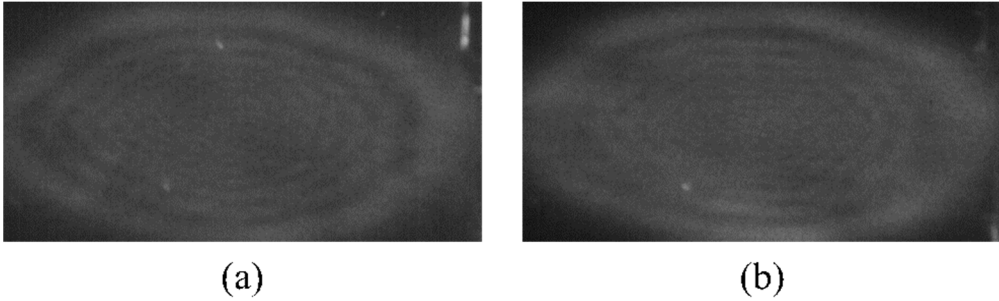


Figure 11. Images of LIF signal with (a) same quartz and (b) 1.1 mm thickness quartz as the upper plate

The comparison of the brightness of the overlapping regions under both conditions suggested that the results of the experiment with the thinner top plate would be about twice as bright as the results with the thicker top plate. If a very thin film like the fuel film if total reflection occurs, you can expect the brightness to double as it is, rather than appear to move as in the above example. Based on this, it was possible to establish the hypothesis that the brightness of the photographed film image is twice as high as the actual brightness. The results of integrated intensity of LIF images verified the hypothesis, as shown in figure 12. The LIF signal intensity of 20 μm thick fuel film resulted in 8,580 with TIR and 4,100 without TIR. The standard deviation is 790 with TIR and 210 without TIR. The area is 37% of the images.

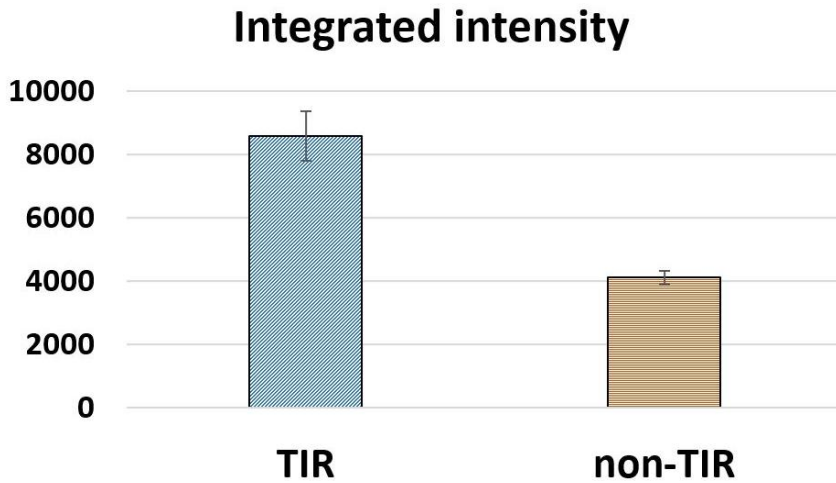


Figure 12. The integrated intensity comparison of central area of LIF images from the setup with TIR and without TIR.

The second experiment was carried out to verify the results of the first experiment. A certain amount of fuel precisely metered with a micro-syringe was applied to the upper surface of the quartz as shown in figure 13. 6 μl of gasoline was released and the average of 5.1 μl was measured at 10 times. A fuel film was formed and filming took less than 0.3 s seconds, which is sufficient time for vaporization to occur, so an approximate understanding of the gasification rate of gasoline is required to be reliable.

After discharging the gasoline to the quartz surface, the fuel film was formed within the shortest possible time. As a result of repeated experiment, a time difference of about 300 ~ 400 ms occurred. To account for the effect of this level of time difference, the fuel film was shot at 5, 245, and 485 ms after injecting the fuel into the injector synchronized with the optical system to determine the tendency of the volume to decrease due to fuel vaporization. If there is a measured value within the range that it can be vaporized during that time, it will mean that the value is not a wrong value.

The third experiment attempts to answer the above questions. The injector is capable of synchronizing the system with repeated injections of relatively precise amounts. The injection signal of the same duration is delivered to the injector to inject the fuel. The fuel volume was measured by taking images of the formed fuel films at 5, 245, and 485 ms after starting the injection signal. As a result represented in figure 14, 5ms and 245ms showed very similar values, but at 485ms they were reduced to 60% of them. Since the power of the laser is controlled to be constant, it can be judged that gasoline has decreased to vaporization. In the previous experiment, gasoline was discharged to the micro syringe and then taken at about 300 to 400 ms, so a volume reduction of about 15 percent was considered to be a reliable experimental value.

As a result of these experiments, we found that the brightness of the image obtained by applying TIR can be made very close to the actual value by reducing it by a factor of magnification.

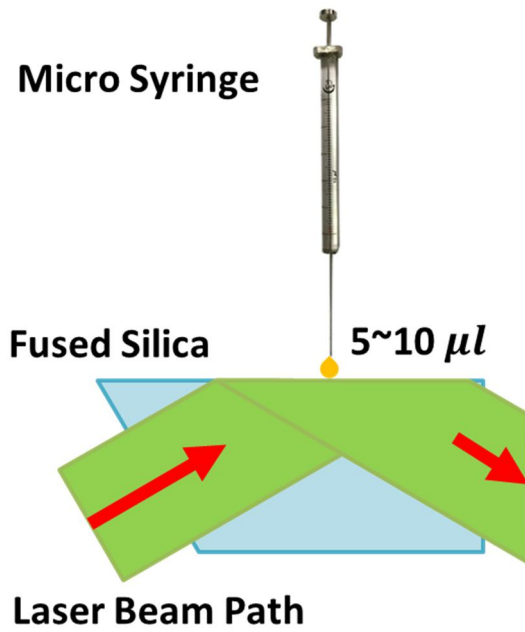


Figure 13. Diagram of experimental setup for confirming the calibration method

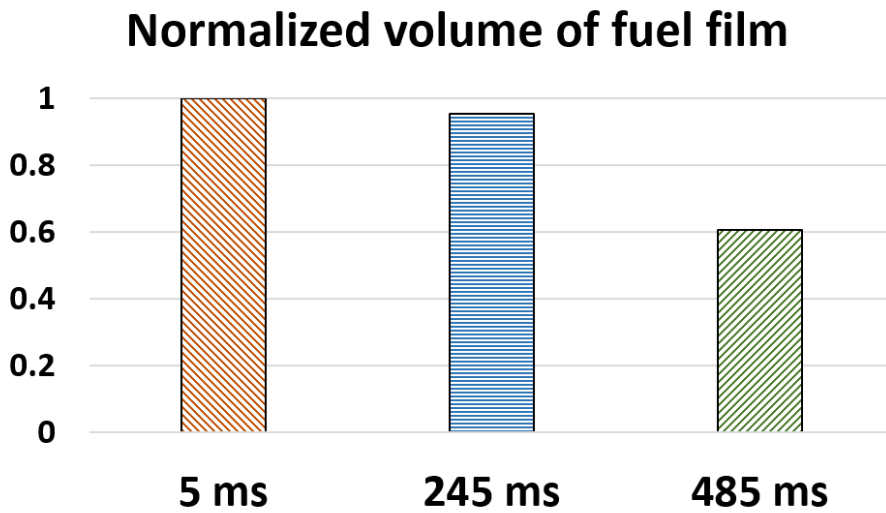


Figure 14. Normalized volume of fuel film under ASOI 5, 245, 485 ms

3.3 Image Processing

3.3.1 Wall film detection

The LIF is emitted in the form of electromagnetic waves and the emission region of the gasoline having various components has such a large region. The electromagnetic waves emitted from the film were recorded on the camera through only the range of 400 nm to 500 nm, which is between 355 nm and 532 nm, the laser wavelength, in order to eliminate interference due to elastic scattering. The camera in charge of recording in the experiment is ICCD and it is very sensitive and has the disadvantage of severe noise as well. In order to achieve accurate quantification as much as possible, only light emission by fuel should be extracted.

The process of the calibration image is as follows.

1. The background images are averaged by averaging the 10 images taken without the fuel liquid film.
2. Based on the background image obtained from 1, the background of the 20 images photographed by each thickness is removed and averaged.
3. Calculate the fitting curve (first order polynomial) for each pixel at the same position in the averaged image of each thickness.

The process of extracting the fuel part is as follows.

1. The background images are averaged by averaging the 10 images taken without the fuel liquid film.

2. Based on the background image obtained in 1, the background of the 20 photographs photographed under each injection condition is removed.
3. In the photographed image, a pixel whose brightness value is larger than a predetermined threshold value is selected as the fuel film region.

The threshold was determined based on the change in mass and area according to the value.

3.3.2 Quantification

Next, the calibration results were applied to calculate the volume. The calculated volume was converted to mass using the density at the temperature conditions.

The process of quantifying the fuel volume and mass is as follows.

1. Reduce the brightness value to 50% in the extracted fuel region image.
2. Based on the background image obtained in 1, the background of the 20 photographs photographed under each injection condition is removed.
3. The calibration data obtained above is used to calculate the thickness by substituting the brightness value of each pixel into the fitting curve.
4. Using the brightness and resolution of each pixel, the area, volume, and mass are derived from the following equations.

For the given volume from the above procedures, the distribution of thickness is expressed as a volume fraction by counting pixels with thickness within a certain

range. This method can be proposed as a tool for new analysis besides simple quantitative comparison or image comparison.

$$A = \sum A_i \quad (4.2.1)$$

$$V = \sum h_i A_i \quad (4.2.2)$$

$$M = \sum \rho_i h_i A_i \quad (4.2.3)$$

Where, A : total area of fuel film
 V : total volume of fuel film
 M : total mass of fuel film
 ρ_i : fuel density of pixel number i
 A_i : fuel film area of pixel number i
 h_i : fuel film mass of pixel number i

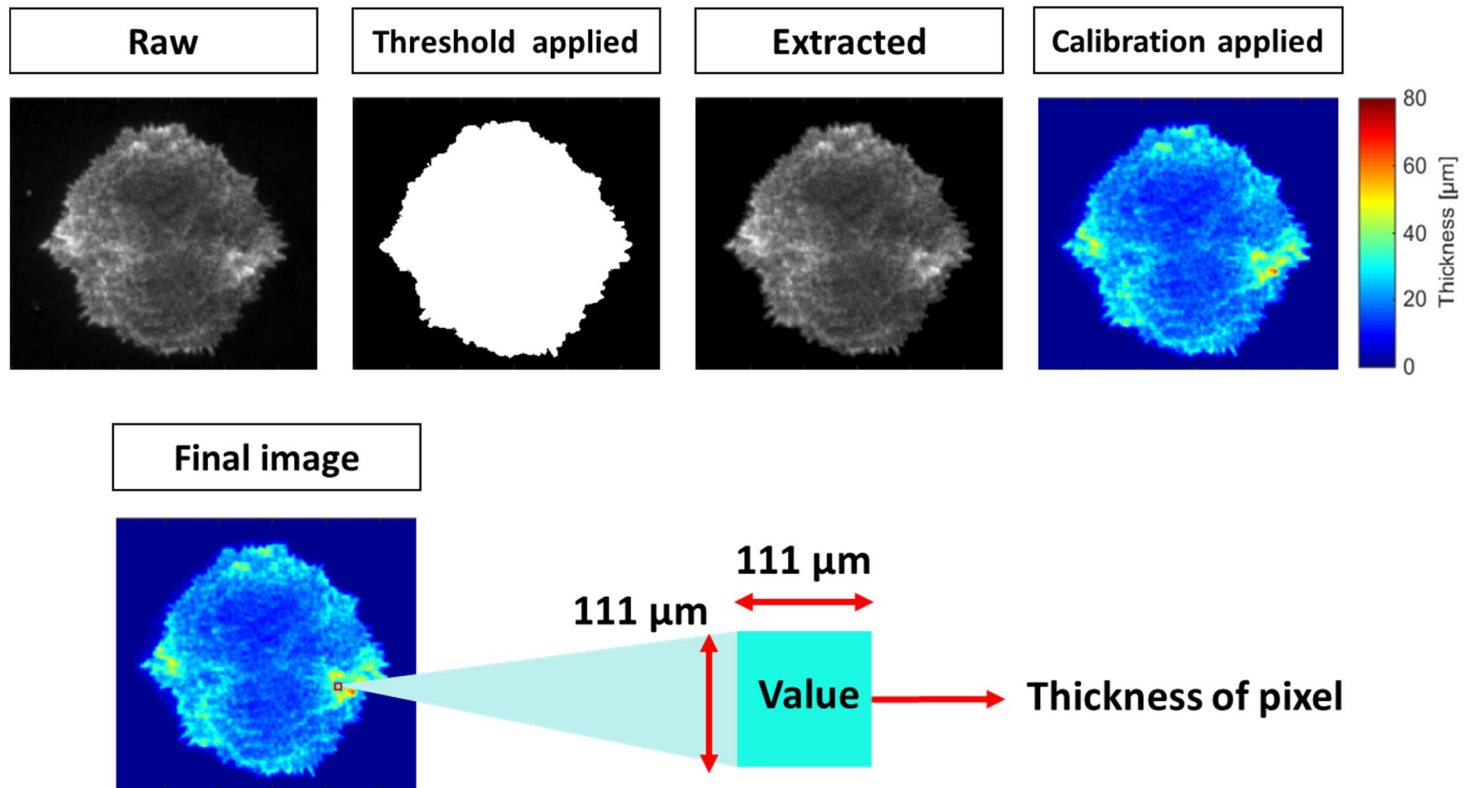


Figure 15. Process of Image processing of liquid fuel film by LIF

Chapter 4. Analysis of Liquid Fuel Films

The experiment was conducted by controlling the impinging angle, injection pressure, split injection, and fuel (tip) temperature conditions. The image recording was repeated 20 times under one condition and analyzed based on the mean value. The deviation means 1 sigma, standard deviation. In this part, only the parts where meaningful results are obtained or the interpretation of the phenomena are included, and the rest of the results are included in the appendix. Based on the mass, area, and volume information calculated from the image processing, the values of each condition were compared and analyzed. Sample pictures representative of each condition are shown in figures 23 and 24.

Figure 16 shows the effect of the remaining conditions on the fuel temperature change conditions that brought about the most significant change. Impinging angle of the results is 90° and almost the same result regardless of the impinging angle. The mass was normalized on the basis of the injected amount of 8.5 mg.

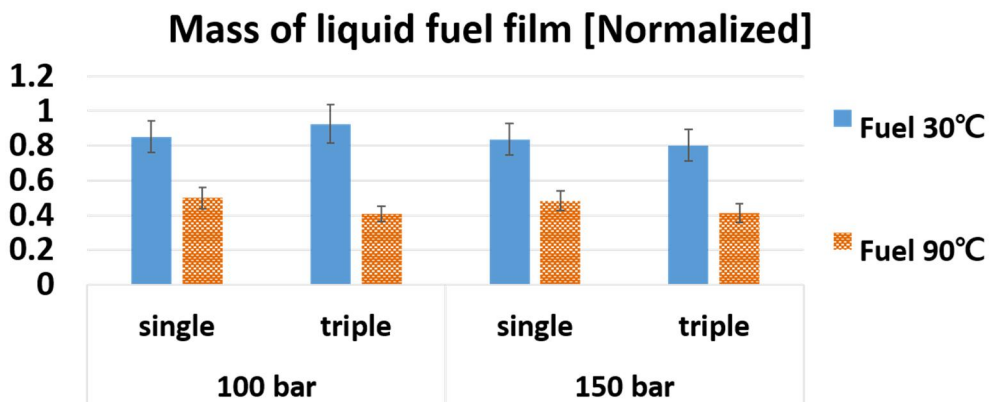


Figure 16. Normalized mass of the liquid fuel film at impinging angle 90°

The change in the fuel temperature had a greater impact on the mass than any other variables. The mass of the film decreased about 40 ~ 50% when the fuel temperature was increased 30 to 90°C. It is known that droplets are split into small pieces due to flash boiling at high temperature, which enhances vaporization of droplets and causes the droplet momentum to decrease [31] .

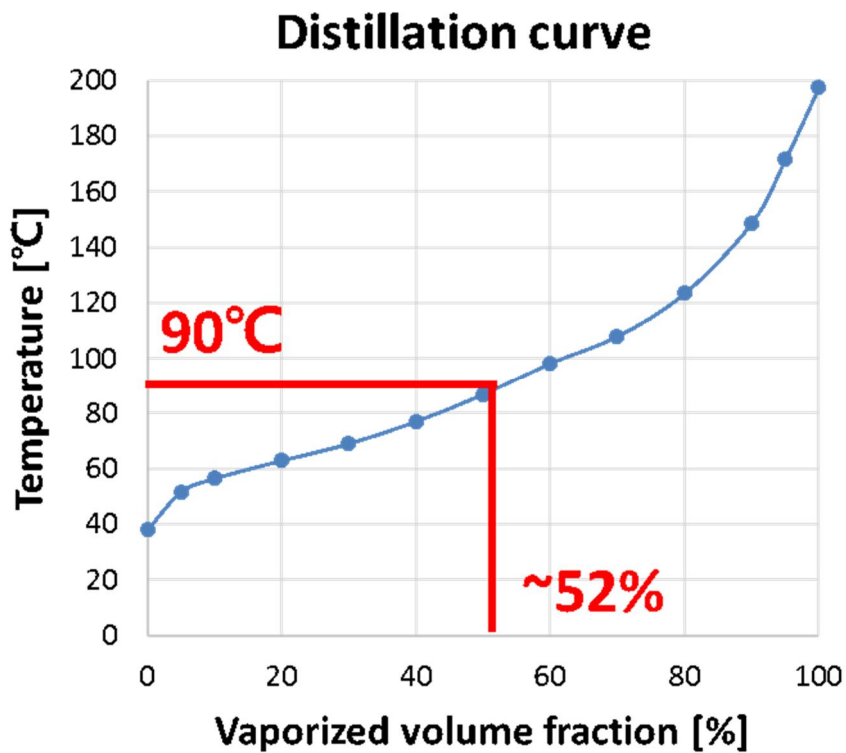


Figure 17. Distillation curve of the gasoline supplied in this experiment

Under flash boiling conditions, the fuel vaporizes rapidly as it exits the nozzle. It is expected that when the droplet reaches the surface, it will vaporize close to the volume corresponding to the initial temperature in the distillation curve. From

figure 17 it is confirmed that the injection temperature of 90°C is the 52% distillation temperature. The results show that the effect of fuel temperature is 41% at 100 bar and 42% at 150 bar. These conclude that the evaporation effect of flash boiling has the greatest effect on reducing the total mass of liquid fuel film.

In contrast to the fuel temperature, the split injection and injection pressures had only a small effect on the deposit mass. Split injection and injection pressure do not have the effect of reducing the amount of fuel reaching the impact surface at a fixed distance. It is presumed that the effect of reducing the exhaust by the split injection is mainly caused by the effect of the delay of the injection due to the effect of the injection delay.

The area was also significantly reduced. Figure 18 shows a 30 percent reduction in area due to temperature increase. The well atomized droplets due to flash boiling could not be thrown away after colliding with the surface. The fuel films of this condition were captured as less splashed images as shown in figure 19.

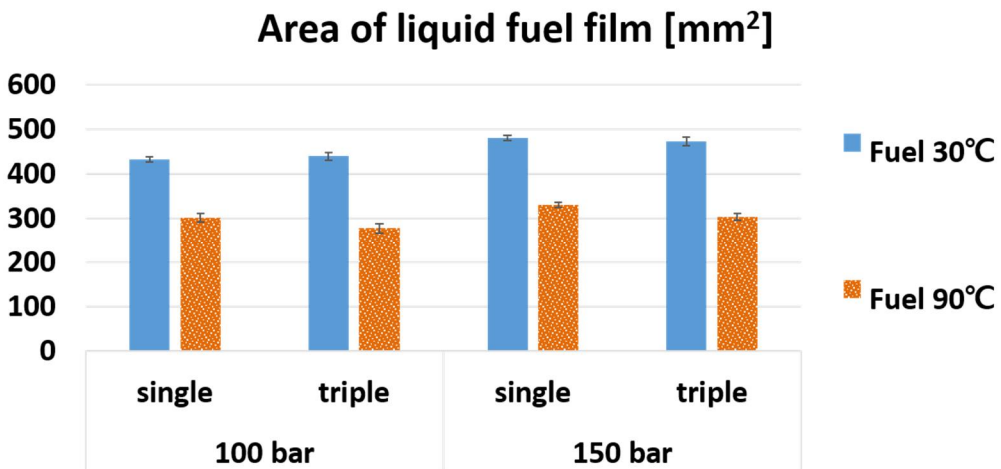


Figure 18. Area of the liquid fuel film at impinging angle 90°

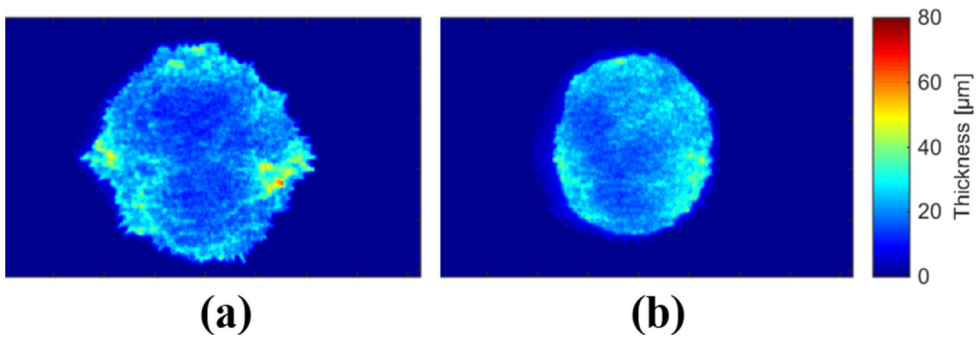


Figure 19. LIF images of liquid fuel film under injection pressure 100 bar, impinging angle 90° , single injection, (a) fuel temperature 30°C and (b) fuel temperature 90°C

From the total fuel film volume and thickness information of each pixel, the thickness distribution in the whole fuel film is expressed in volume fraction as shown in figure 20. The error bar means 1 sigma and is the result that is averaged 20 times. It is appropriate to compare the thicker region because it is highly likely that the thicker region is detrimental to vaporization and become a residual fuel film.

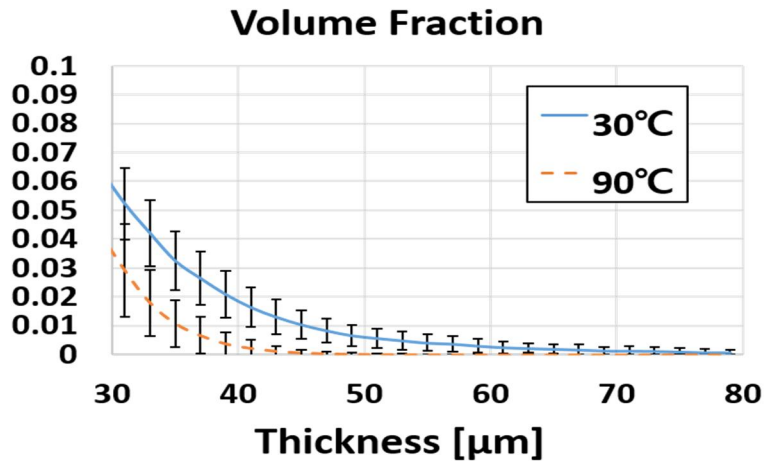


Figure 20. Volume fraction of liquid fuel film thickness over 30 microns at 90°

When the fuel temperature is 90°C, the volume fraction of more than 30 microns in thickness is significantly reduced. The actual volume is larger because the total volume is also reduced. When the fuel temperature is high, not only the effect of simply increasing the mass, but also the thickness distribution is formed favorably for vaporization. From the viewpoint of combustion, it can be said that a high-temperature fuel is a better condition than a low-temperature fuel.

Figures 21 and 22 are graphs of mass and area comparisons for collision angles. It is generally believed that a smaller amount of fuel will be deposited at a impinging angle of 45 degrees. Experimental results prove that such ideas are partially correct. When the impinging angle was tilted at 45 degrees, the mass was reduced by about 25 to 30 percent and the area was reduced by 20 to 25 percent.

Mass of liquid fuel film [Normalized]

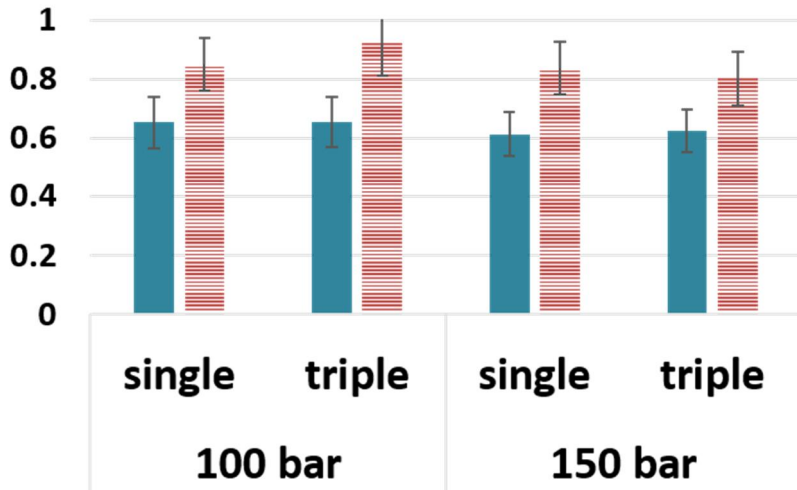


Figure 21. Normalized mass of the liquid fuel film at fuel temperature 90°C

Area of liquid fuel film [mm²]

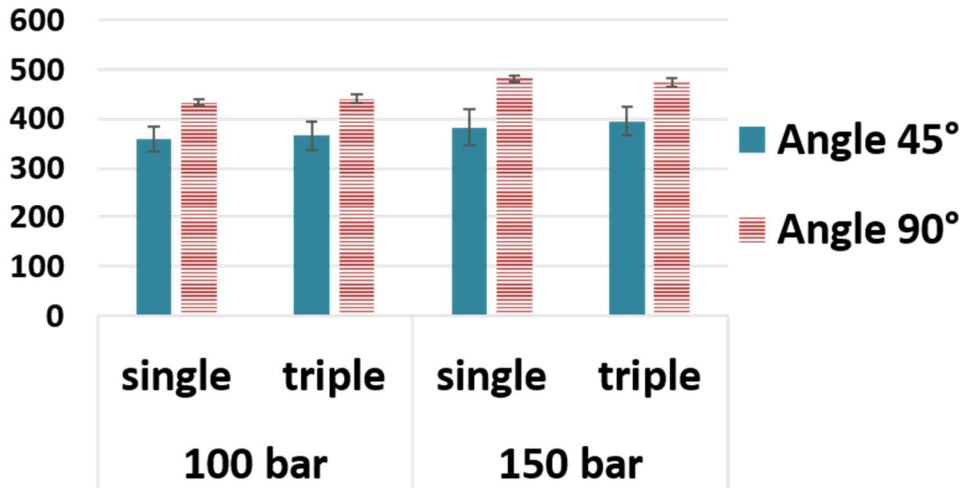


Figure 22. Area of the liquid fuel film at fuel temperature 90°C

The droplets that collide at an oblique angle also have a tangential momentum as much as the normal momentum. The smaller normal momentum lowers the probability that droplets adhere on the wall after collision, increasing the likelihood of rebound interaction [28]. The tangential moment causes the droplet to move in the tangential direction of the movement path even after collision, so droplets are directed farther from the initial position on the surface. This spray-wall interaction explains that spraying at an oblique angle with the impact surface is more beneficial in fuel vaporization and mixing. However, if the thickness distributions of the two conditions with the previously described method are compared, it is suggest that the tilted angle is not prior to the perpendicular.

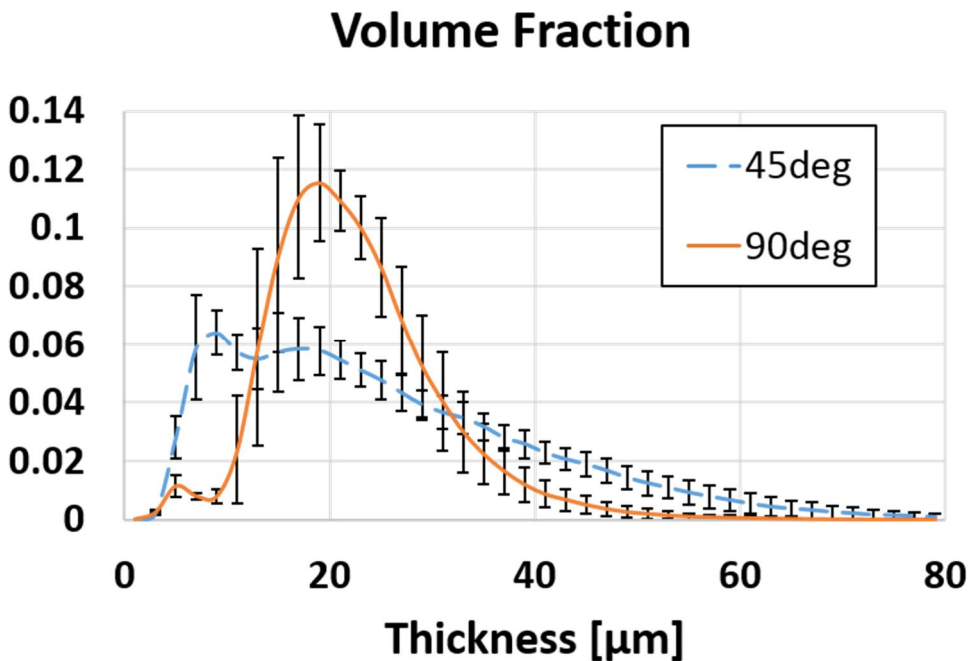


Figure 23. Volume fraction of liquid fuel film thickness overall thickness at 90°C

In the figure 23, the dash line shows a collision angle of 45 degrees and the solid line shows a impinging angle of 90°. In the case of 90°, thickness distribution is around 20 microns and has a Gaussian distribution shape. Such a shape is convincing because it is the spray wall interaction of a large number of vertically colliding droplets.

The fuel film of impinging angle 45° is more evenly distributed than that of 90°. This means that the thickness of the fuel film is varied from a thick part to a thin part. A remarkable point of results is that the region with a thickness of 30 microns or thicker is much more at the impinging angle 45° than at the impinging angle 90°. The difference is greater than the reduced total mass of 25%. From this, it has been found that the inclined impinging angle is not a convincing condition for making a film favorable to combustion.

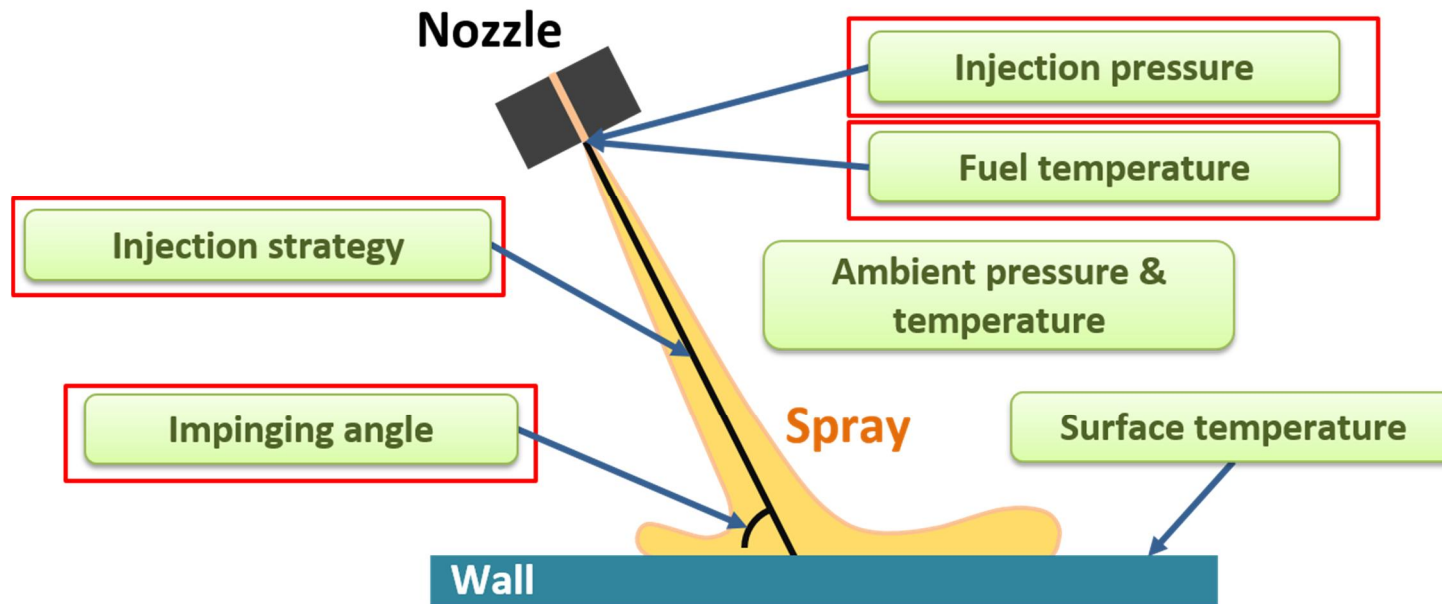


Figure 24. Injection conditions and ambient conditions that may affect fuel film formation and the conditions controlled in this study (framed boxes)

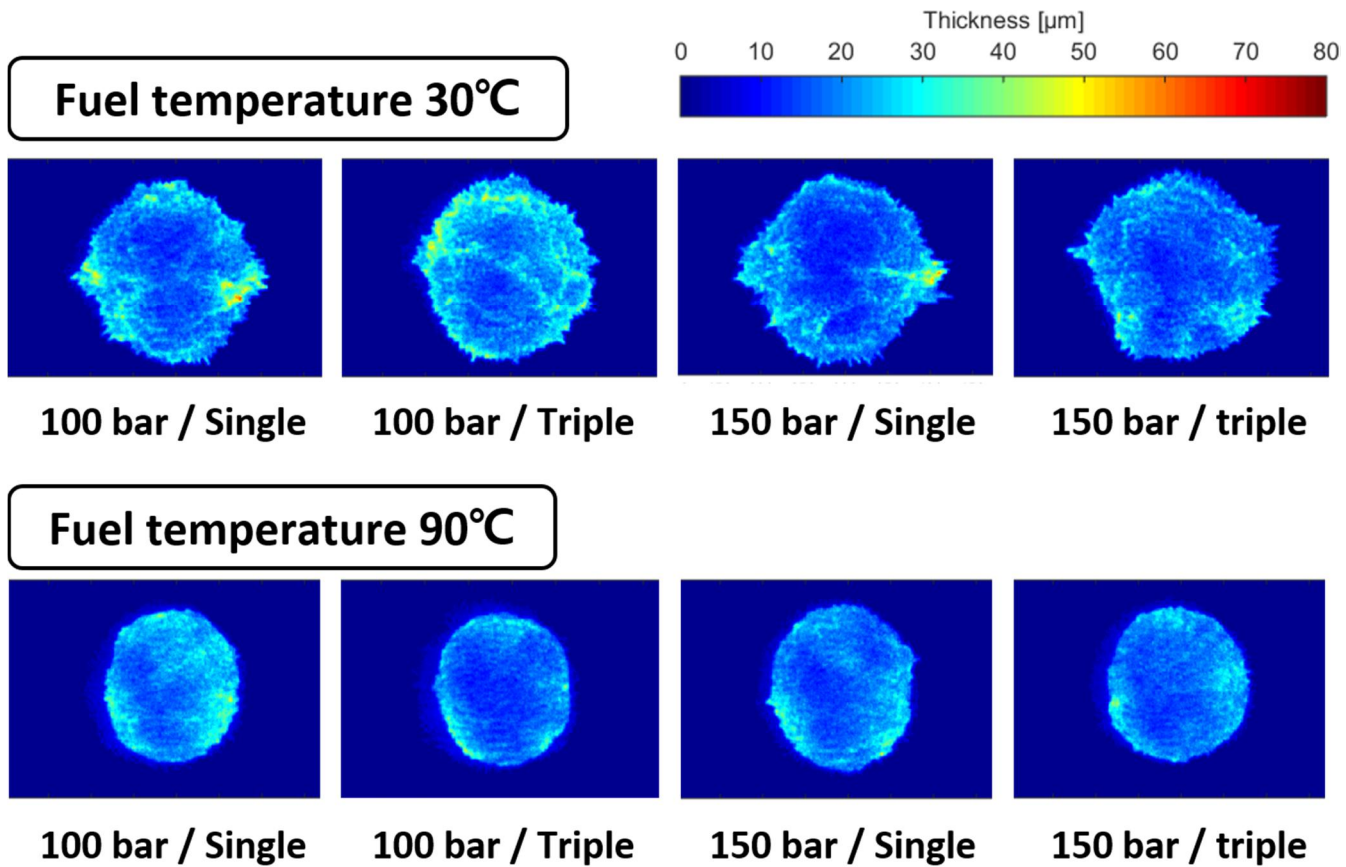


Figure 25. Sample images of liquid fuel film under several injection conditions at 90° impinging angle

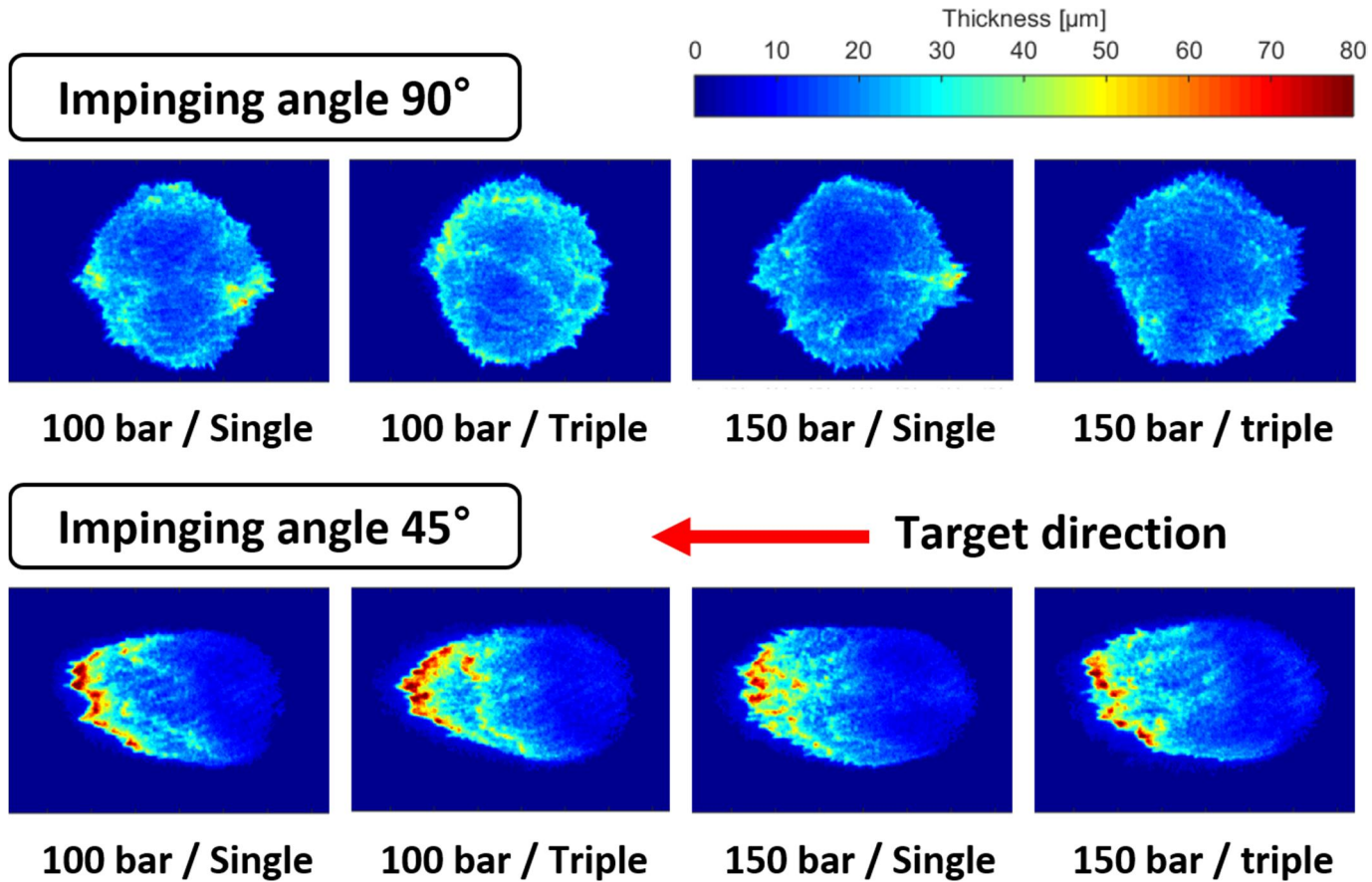


Figure 26. Sample images of liquid fuel film under several injection conditions at 30°C fuel (tip) temperature

Chapter 5. Conclusions

The three major accomplishments of this study are as follows

1. The effectiveness of LIF with TIR on preventing the laser from absorbing into the airborne droplets above the fuel film was evaluated.
2. The previous calibration method was applied to TIR LIF for Quantitative measurement of liquid fuel film.
3. The empirical results of mass, area and the thickness distribution of the fuel film were analyzed to find the condition that has the most significant amount of effect on the formation of the fuel film.

It has been recovered as a problem of LIF for a while and it is confirmed that it causes error. As a solution, TIR was proposed and applied, and measurement was performed, but its effect was not confirmed. In this research, The image of the gasoline spray on the way to the collision is the basis for judging whether the LIF signal is emitted from the spray. As shown in figure 8, no spray was detected under TIR conditions.

A calibration method was applied to quantify the intensity of the LIF signal emitted by irradiating the laser after filling the gap with the guaranteed thickness gauges. This setup differs from the conditions under which LIF occurs in actual fuel films. TIR caused the fuel film to release LIF twice. The path of the laser is through a film that is twice as thick. It was verified from the brightness of the images in both situations.

The LIF of the fuel film formed by changing injection pressure, split injection, fuel temperature, impinging angle was recorded as an image. The mass, area, and thickness distribution of the fuel film were determined by quantification method. Injection pressure and split injection do not have a great effect on the fixed system. The elevated fuel temperature promoted the vaporization and atomization of the fuel and suppressed the formation of the fuel film. The formed fuel film is uniform in thickness and is considered to be advantageous for vaporization. Impinging angle is a major factor affecting the shape of the fuel film. The mass and area are reduced and the thickness distribution has a totally different shape of graph. The thickness of the collision point was very thin, but the ratio of the thick part was relatively high due to the accumulated fuel in the injected direction.

Bibliography

1. Kasseris, E. and J.B. Heywood, *Charge Cooling Effects on Knock Limits in SI DI Engines Using Gasoline/Ethanol Blends: Part 1-Quantifying Charge Cooling*. 2012, SAE International.
2. Iwamoto, Y., et al., *Development of Gasoline Direct Injection Engine*. 1997, SAE International.
3. Bertsch, M., T. Koch, and A. Velji. *Influence of charge motion and injection pressure on the particulate emission of a gasoline DI-SI engine at homogeneous, boosted operation*. in *SIA Powertrain Conference: The low CO2 spark ignition engine of the future and its hybridization*. 2015.
4. Mitroglou, N., et al., *Spray characteristics of a multi-hole injector for direct-injection gasoline engines*. *International Journal of Engine Research*, 2006. 7(3): p. 255-270.
5. Drake, M.C., et al., *Piston fuel films as a source of smoke and hydrocarbon emissions from a wall-controlled spark-ignited direct-injection engine*. 2003, SAE Technical Paper.
6. *Euro 5/6 standards (2009/2014): Regulation 715/2007 and several comitology regulations.*; Available from: Available from: <http://www.dieselnet.com/standards/eu/ld.php>.
7. Choi, K., et al., *Size-resolved engine exhaust aerosol characteristics in a metal foam particulate filter for GDI light-duty vehicle*. *Journal of Aerosol science*, 2013. 57: p. 1-13.
8. Ramadhas, A., et al., *Impact of Ambient Temperature Conditions on Cold Start Combustion, Gaseous and Particle Emissions from Gasoline Engines*. 2017, SAE Technical Paper.

9. Saliba, G., et al., *Comparison of Gasoline Direct-Injection (GDI) and Port Fuel Injection (PFI) Vehicle Emissions: Emission Certification Standards, Cold-Start, Secondary Organic Aerosol Formation Potential, and Potential Climate Impacts*. Environmental science & technology, 2017. **51**(11): p. 6542-6552.
10. Yang, J. and L.A. Melton, *Fluorescence-based method designed for quantitative measurement of fuel film thickness during cold-start of engines*. Applied Spectroscopy, 2000. **54**(4): p. 565-574.
11. Maligne, D. and G. Bruneaux, *Time-resolved fuel film thickness measurement for direct injection SI engines using refractive index matching*. 2011, SAE Technical Paper.
12. Pan, H., et al., *Experimental Investigation of Fuel Film Characteristics of Ethanol Impinging Spray at Ultra-Low Temperature*. 2017, SAE Technical Paper.
13. Cho, H. and K. Min, *Measurement of liquid fuel film distribution on the cylinder liner of a spark ignition engine using the laser-induced fluorescence technique*. Measurement Science and Technology, 2003. **14**(7): p. 975.
14. Alonso, M., et al., *A laser induced fluorescence technique for quantifying transient liquid fuel films utilising total internal reflection*. Experiments in fluids, 2010. **48**(1): p. 133-142.
15. Schulz, F., et al., *Systematic LIF fuel wall film investigation*. Fuel, 2016. **172**: p. 284-292.
16. Schulz, F. and J. Schmidt. *Investigation on fuel wall films using laser-induced fluorescence*. in *DIPSI Workshop 2012. Droplet Impact Phenomena & Spray Investigations*. 2012. Università degli studi di Bergamo.
17. Schulz, F., J. Schmidt, and F. Beyrau, *Development of a sensitive experimental set-up for LIF fuel wall film measurements in a pressure vessel*. Experiments in Fluids, 2015. **56**(5): p. 98.

18. Henkel, S., et al., *Novel method for the measurement of liquid film thickness during fuel spray impingement on surfaces*. Optics express, 2016. **24**(3): p. 2542-2561.
19. Drake, M.C., T.D. Fansler, and M.E. Rosalik. *Quantitative high-speed imaging of piston fuel films in direct-injection engines using a refractive-index-matching technique*. in *15th Annual Conference on Liquid Atomization and Spray Systems, Madison, WI*. 2002.
20. Yang, B. and J. Ghandhi, *Measurement of diesel spray impingement and fuel film characteristics using refractive index matching method*. 2007, SAE Technical Paper.
21. Kay, P.J., et al. *Development of a 2D quantitative LIF technique towards measurement of transient liquid fuel films*. in *10th international congress on liquid atomisation and spray systems, Kyoto, Japan*. 2006.
22. Rincon, M.A.A., *Novel PLIF techniques for analysis of G-DI spray dynamics*. 2009: Cardiff University (United Kingdom).
23. Kashdan, J.T., *Tracer LIF visualisation studies of piston-top fuel films in a wall-guided, low-NOx diesel engine*. 2008, SAE Technical Paper.
24. Schulz, C. and V. Sick, *Tracer-LIF diagnostics: quantitative measurement of fuel concentration, temperature and fuel/air ratio in practical combustion systems*. Progress in Energy and Combustion Science, 2005. **31**(1): p. 75-121.
25. Schulz, F. and J. Schmidt. *Infrared thermography based fuel film investigations*. in *12th Triennial International Conference on Liquid Atomization and Spray Systems, Heidelberg, Germany*. 2012.
26. Schulz, F., et al., *Gasoline wall films and spray/wall interaction analyzed by infrared thermography*. SAE International Journal of Engines, 2014. **7**(2014-01-1446): p. 1165-1177.
27. Schulz, F. and F. Beyrau, *The influence of flash-boiling on spray-targeting and fuel film formation*. Fuel, 2017. **208**: p. 587-594.

28. Mahulkar, A.V., G.B. Marin, and G.J. Heynderickx, *Droplet–wall interaction upon impingement of heavy hydrocarbon droplets on a heated wall*. Chemical Engineering Science, 2015. **130**: p. 275-289.
29. *FUSED QUARTZ AVERAGE TRANSMITTANCE CURVES*. Available from: http://www.technicalglass.com/fused_quartz_transmission.html.
30. Kull, E., et al., *Two-dimensional visualization of liquid layers on transparent walls*. Optics letters, 1997. **22**(9): p. 645-647.
31. Sher, E., T. Bar-Kohany, and A. Rashkovan, *Flash-boiling atomization*. Progress in Energy and Combustion Science, 2008. **34**(4): p. 417-439.

국문 초록

직접 분사 스파크 점화 엔진에서는 연소실 내로 연료를 직접 분사하여 연료가 기화될 때 발생하는 차지쿨링 효과를 극대화하여 높은 체적 효율을 확보하고 압축비를 높일 수 있다. 이런 효과로부터 엔진의 출력은 유지한 채 크기를 줄이는 다운사이징이 가능하다. 다운사이징으로 줄어든 무게와 열 손실은 연료 소비 효율을 개선시키고 결과적으로 CO₂ 배출이 감소한다. 이러한 장점을 바탕으로 직접 분사 엔진의 점유율이 빠르게 늘어나고 있다. 한편, 직접 분사 엔진의 구조상 연소실 내부로 분사된 연료가 피스톤이나 실린더 벽면에 도달하기 쉬워졌다는 단점도 있다. 연료가 완벽하게 기화되지 않거나 연료 막으로 남게 되면 국부적으로 연료가 농후한 지역을 형성하고 연소에 악영향을 끼쳐 불완전 연소와 입자상 물질 배출의 원인이 된다. 점차 엄격해지는 배기 규제에 대응하기 위해 배기 물질의 형성 원인인 연료 막 생성을 최대한 억제해야 한다. 피스톤과 실린더에 잔류하는 연료를 효율적으로 저감하기 위해서는 연료 막의 형성과 기화 과정에 대한 충분한 이해가 필요하다.

연료 막 형성에 영향을 미치는 인자들에 대해 알아보고자 레이저 유도 형광법을 이용하여 직접 분사 스파크 점화 엔진에서 연료 막에 대한 정량적인 계측 연구를 수행하였다. 내부전반사로 레이저의 경로를 제한하여 연료 막 위의 공기 중 연료 액적들의 형광이 일어나지 않도록 하였다. 이 연구의 결과로 연료 막의 형성에 영향을 미치는 인자들에 대한 이해도를 높이고 연료 막 모델링에 기반 자료를 제공할 수 있다.

내부전반사를 이용했던 기존 연구들을 바탕으로 실험을 진행하던 중 레이저 펄스가 내부전반사가 일어나면 연료 막을 두 번 투과하게 된다는 사실을 발견했다. 연료 막은 두 배의 레이저 펄스 에너지를 흡수할 것이고

그만큼 더 큰 형광 신호가 방출된다. 이러한 점을 고려하여 두께 게이지를 이용한 정량화 과정을 진행하였고 성공적으로 연료 막을 정량화 할 수 있었다.

이 연구에서는 기존 연구들에서 논의되지 않았던 연료 막 내의 두께 분포에 대한 분석을 시도하였다. 그 동안 시도하지 않았던 연료 온도에 따른 연료 막 형성 특성도 관찰하고자 하였다. 연료 막의 질량, 면적, 두께 분포의 결과를 종합하여 연료 막 형성에 가장 중요한 인자를 밝혀내고자 하였다.

분사 압력과 다단 분사는 고정된 시스템에서는 큰 효과를 내지 못하였다. 연료 온도의 증가는 연료 막 형성에 가장 큰 효과를 가져왔다. 연료의 온도를 섭씨 30도에서 90도로 증가시켰을 때 연료의 질량과 면적은 40~50% 감소하였고 더 균일한 두께의 막이 형성되었다. 벽면과의 충돌 각도 또한 연료 막 특성에 주요한 영향을 미쳤다. 수직으로 벽에 부딪힐 때보다 45° 기울어져서 부딪힐 때 연료 막의 질량이 25~30% 감소하였다. 충돌 방향으로 축적된 연료에 의해 연료 막 내의 두께가 다양하게 분포하는 형상이 보였다. 이러한 결과는 연료가 두껍게 막을 형성하고 있는 것이 기화에 불리하므로 경사지게 충돌하는 것이 연소에 유리하다고 단정지을 수는 없는 근거가 될 수 있다.

주요어: 가솔린 직분사, 레이저 유도 형광, 연료 액막 계측, 내부전반사

학번: 2016-20704

